Blue-light (488 nm) -irradiation-induced photoactivation of the photoactivatable green fluorescent protein

Ilaria Testa, Davide Mazza, Sara Barozzi, Mario Faretta, and Alberto Diaspro

Citation: Applied Physics Letters **91**, 133902 (2007); doi: 10.1063/1.2790847
View online: http://dx.doi.org/10.1063/1.2790847
View Table of Contents: http://scitation.aip.org/content/aip/journal/apl/91/13?ver=pdfcov
Published by the AIP Publishing

Blue-light (488 nm)-irradiation-induced photoactivation of the photoactivatable green fluorescent protein

Ilaria Testa and Davide Mazza
LAMBS-MicroScoBio, Department of Physics, University of Genoa, I-16146 Genoa, Italy

Sara Barozzi and Mario Faretta
Department of Experimental Oncology, European Institute of Oncology, 20141 Milan, Italy

Alberto Diaspro[a)]
LAMBS-MicroScoBio, Department of Physics, University of Genoa, I-16146 Genoa, Italy, Istituto FIRC di Oncologia Molecolare (IFOM), 20139 Milan, Italy and IBF-CNR, National Research Council, I-16149 Genoa, Italy

(Received 3 August 2007; accepted 10 September 2007; published online 26 September 2007)

We experimentally demonstrate the photoactivatable green fluorescent protein (paGFP) photoactivation in a wavelength range where the molecule barely absorbs. The photoactivation is induced at the same wavelength used to visualize the activated form of paGFP. This can be an obstacle in the intensity evaluation in photoactivation experiments. Power and kinetics based characterization of the effect was performed in model and cell systems. This study shows an operative threshold in which paGFP is not subjected to significant photoconversion. 488 nm photoactivation is in tune with the broadening of the paGFP two-photon activation spectrum, indicating that multiple interactions lead to modifications of the molecular structure and alterations of its photophysical properties. © *2007 American Institute of Physics*. [DOI: 10.1063/1.2790847]

Besides techniques such as fluorescence recovery after photobleaching, photoactivation techniques are becoming more and more popular as a tool to analyze molecular dynamics in living cells.[1,2] Photoactivatable green fluorescent protein (paGFP) is a GFP variant obtained by targeted point mutation whose photophysical properties can be easily manipulated to highlight selected regions through controlled exposure of high photon energy density flux. paGFP is normally excited at near UV wavelength (405 nm), with an emission peak centered at 520 nm. Absorption cross section at 488 nm is low in the not-activated form. However, when irradiated with high-energy fluxes at 405 nm, the protein shows a dramatic change in its absorption spectra, becoming efficiently excitable at 488 nm.[3] paGFP also exhibits a two-photon absorption spectrum in the red spectral range between 750 and 820 nm making it possible to employ two-photon microscopy to induce photoactivation.[4]

Photoactivation experiments have been consequently employed to track the movement of selected structures in cells[5] or specific cells in organisms[6,7] while the redistribution of the fluorescence signal of activated molecules has been efficiently used for protein diffusion measurements.[8]

A photoactivation protocol is generally composed of three phases, namely, a preactivation imaging step for recording of the initial state employing 488 nm excitation, a photoactivation step characterized by energy irradiation with full power laser illumination of the region of interest, and a postactivation imaging step to follow the spatial distribution of the photoactivated molecules over time. Particularly, in the case of diffusion coefficient measurements or quantitative fluorescence imaging, the setting of correct imaging conditions is fundamental to obtain a maximized signal-to-noise ratio. As well, 488 nm illumination parameters must be appropriately set to minimize bleaching conditions.

We realized the above-mentioned protocol using an imaging device, Olympus FV1000 confocal microscope equipped with an immersion oil apochromat 60× 1.42 numerical aperture (NA) objective. paGFP-H2B fusion protein was expressed in human HeLa cells grown on glass coverslips under standard cell culture conditions. Laser intensities at the sample, I, are calculated as described in Habuchi *et al.*[9]

Figure 1 clearly shows the paGFP photoproduct dependence on the imaging energy parameters. It appears that by employing a moderate 488 nm irradiation ($I=0.57$ MW/cm^2) for fluorescence imaging of the photoactivated molecules, a tenfold increase in terms of activation efficiency is gained against a fourfold increase observed at higher 488 nm irradiation ($I=5.37$ MW/cm^2). Since the occurrence of a photobleaching process of the photoactivated molecules can hardly explain the observed behavior, we hypothesized a possible photoconversion effect due to the 488 nm imaging step. Figure 2 clearly demonstrates that blue light (488 nm) illumination is able to induce photoconversion of native paGFP. In fact, high-energy irradiation with blue light, obtained by zooming in on the region of interest, clearly evidenced a net increase in fluorescence in the postactivation observation. We observed the very same effect on purified paGFP molecules immobilized on sepharose beads using a Leica TCS SP2 AOBS confocal microscope equipped with 100× oil 1.4 NA objective HCX PL APO, evidencing that photoactivation with visible light is not due to protein modifications caused by cell environment.

The photophysical properties of paGFP activated by blue light illumination were checked by recording the emission spectra of the activated molecules [Fig. 2, graph (b)] that exhibited a fluorescence emission peak at 520 nm wave-

[a)]Author to whom correspondence should be addressed. Tel.: +390103536426. Electronic mail: diaspro@fisica.unige.it

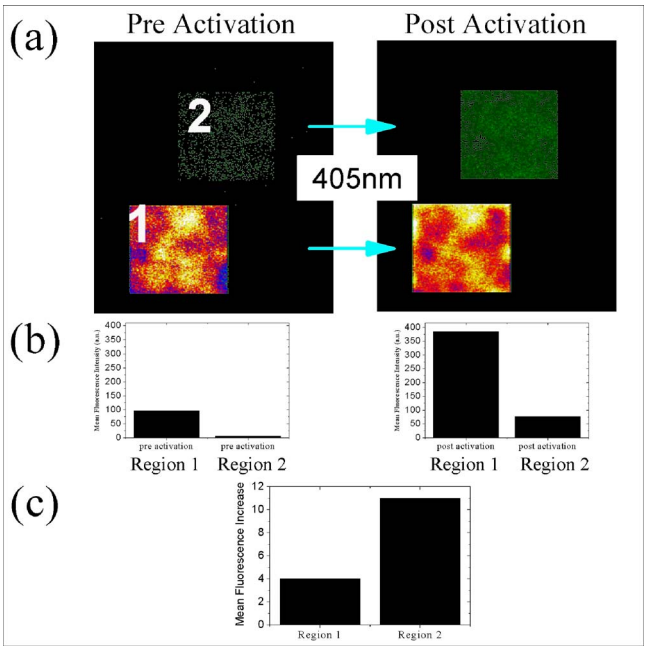

FIG. 1. (Color online) Photoactivation dependence on imaging conditions. (a) The pre- and postactivation images were collected exciting only the square regions 1 and 2 at 488 nm, respectively, at $I=5.37$ MW/cm^2 and $I=0.57$ MW/cm^2 of mean laser intensity delivered on the sample. The activation step was performed using the same parameters in both regions: $I=3.7$ MW/cm^2, $\lambda=405$ nm, pixel dwell time=4 μs, and pixel size=37 nm. (b) The histograms show the mean fluorescence intensity collected in the selected cell's regions of the pre- and postimages. (c) By dividing the fluorescence intensity collected in the postactivation images and the preactivation image, respectively, for regions 1 and 2, we reported in the histogram the increase of fluorescence induced by photoactivation of paGFPs.

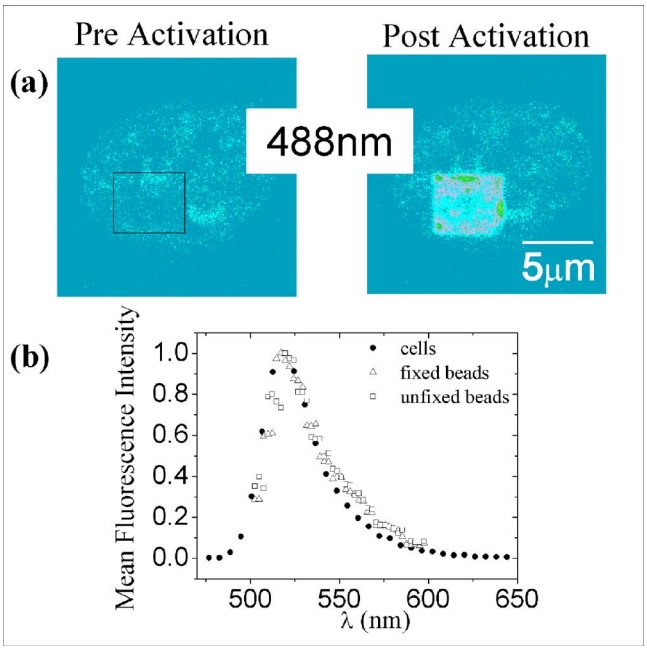

FIG. 2. (Color online) Observation and characterization of 488 nm activation. (a) Preactivation and postactivation images were collected at low excitation intensity at 488 nm excitation wavelength ($I=0.13$ MW/cm^2); the activation was performed in the region of 21.16 μm^2 under high excitation power at 488 nm ($I=0.95$ MW/cm^2). The experiment was performed on fixed HeLa cells expressing paGFP-H2B fusion protein (b) Emission spectra of activated paGFP at 488 nm as excitation wavelength ($I=0.13$ MW/cm^2), collected in three different samples: fixed HeLa cells expressing the vector paGFP-H2B, and fixed and unfixed sepharose beads with purified paGFP immobilized on the surface.

length, as expected for "classical" violet light (405 nm) induced photoactivation.

Such a surprising activation can consequently effect a rise in "background fluorescence" influencing the temporal analysis of fluorescence redistribution of activated regions and leading to incorrect estimation of molecular diffusion coefficients. To further investigate the possibility that imaging conditions normally employed in photoactivation protocols could lead to unexpected 488 nm induced photoactivation, we imaged single cells expressing the nuclear paGFP-H2B fusion protein at different illumination powers without any exposure to violet light and monitored the behavior of the emitted fluorescence over time (Fig. 3). As a function of the excitation intensity, different mono- and biphasic curves were measured: high laser intensity firstly induced increase of mean fluorescence on the observed nuclei, reaching a maximum value, followed by a second phase during which photobleaching prevails, inducing a progressive reduction in the observed signal (Fig. 3, $I=0.95$ MW/cm^2). Progressive reduction of the illumination intensity exhibited a slow down in the activation process causing a delayed maximal activation before the onset of the phase dominated by photobleached paGFP molecules. It is worth noting that low power 488 nm excitation extends the duration of the activation phase to extremely long periods with a progressive increase in the detected signal (Fig. 3, $I=0.38$ MW/cm^2). Furthermore, we identified an intensity range in which no evidence of photoactivation and photobleaching was detected for a long observation period. This is the range to be used in order to analyze the photophysical and kinetic behavior of activated molecules without additional perturbation of the fluorescent properties of the molecules.

We used this setting to analyze the photophysical and kinetic behavior of photoactivation induced in the 0.13–5.37 MW/cm^2 intensity range, employing an acousto-optic tunable filter to rapidly modulate irradiation in spatially selected target regions while maintaining laser intensity for imaging below the identified operative threshold [Fig. 4, graph (a)].

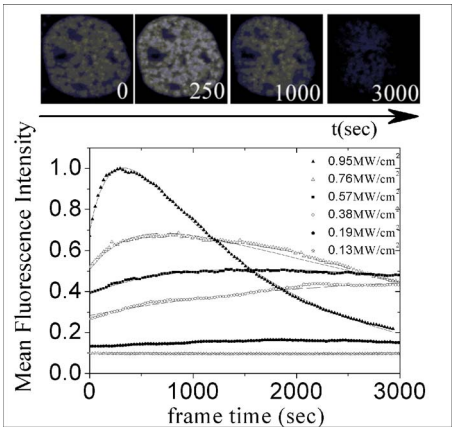

FIG. 3. (Color online) Activation kinetics under 488 nm illumination. We show six curves for different 488 nm laser intensities within the range of 0.13–0.95 MW/cm^2. The ordinate values represent the mean fluorescence intensity emitted by paGFP molecules inside the nucleus as a function of the irradiation time. The curves are normalized to the highest intensity value obtained by illuminating at 0.95 MW/cm^2. Each activation pulse was performed with pixel dwell time=1 ms and pixel size=68 nm.

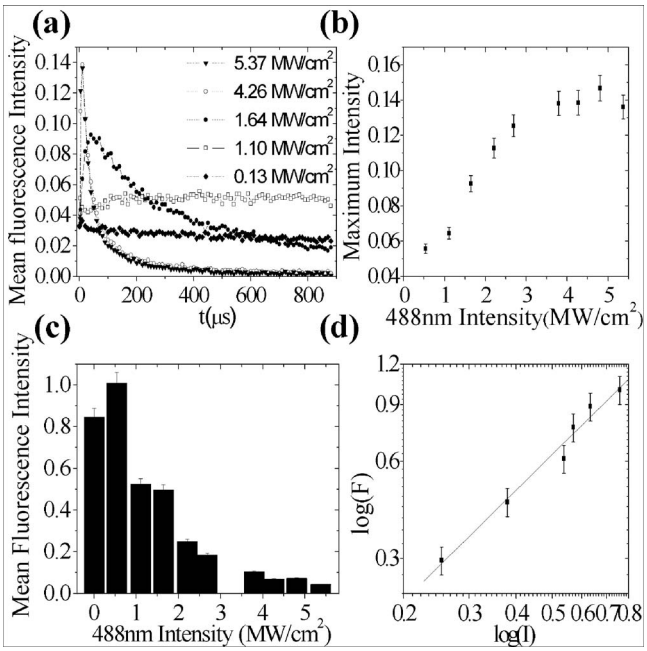

FIG. 4. Characterization of visible activation respect to the UV-vis activation. (a) The mean fluorescence intensity collected in square regions of the cell nucleus observed at 488 nm low intensity (I=0.13 MW/cm^2) and activated at different 488 nm laser intensities within the range of 1.10–5.37 MW/cm^2 with sequential pulses with pixel dwell time of 2 μs and pixel size of 37 nm. On the time scale is shown the cumulative activation time per pixel. (b) Different maxima reached from each curve until an evidence of saturation. The maximum value reached activating at 405 nm is normalized at 1 and used as reference in order to compare UV-vis irradiation photoproduct with respect to the visible one. (c) Recovery of fluorescence obtained in regions of the cell illuminated at several 488 nm laser line intensities at several powers and subsequently irradiated with a short pulse at 405 nm UV-vis. The visualization was performed at 488 nm with an average intensity of I=0.13 MW/cm^2. These values are shown in the histogram for all the activation visible power analyzed. (d) The graph shows the visible activation process dependence on the power. The mean fluorescence intensity values, collected on 4.6×4.6 μm^2 regions of the bead model system activated at different 488 nm laser line intensities, were visualized in a bilogarithmic as function of laser intensity. Black line represents the linear fit of the data with a slope of 1.1±0.1.

The observed behavior suggests that 488 nm light induced photoproducts result from two competing processes, namely, activation of native paGFP molecules and photobleaching. Due to this competition, the activation efficiency exhibited a saturation effect suggesting that only a fraction of molecules can be photoconverted leading to a fold increase that is about 15% of the maximal 405 nm induced activation [Fig. 4, graph (b)].

To verify the assumption of a photoactivation limited to a variable fraction of molecules the blue light activated regions were subjected to high intensity 405 nm irradiation (I=3.7 MW/cm^2) and the resulting increase in signal due to the residual photoactivation process was measured.

Recovery of fluorescence reaches different values depending on the 488 nm illumination intensity employed in the first activation step, as shown in the histogram of Fig. 4, graph (c). All the measured fluorescence signals were normalized to the maximum increase of fluorescence obtained by activating a region of the nucleus at 405 nm. The progressive decrease in the recovered fluorescence with increasing 488 nm activation intensity demonstrates the coexistence of photoactivation and photobleaching which inevitably depletes the number of paGFP molecules in the native state.

To complete the characterization of the blue light induced activation process, the increase in the fluorescent signal brought by a short pulse (pixel dwell time of 4.9 μs, pixel size of 9 nm, I=0.25–0.75 MW/cm^2) of 488 nm light at different laser powers was measured [Fig. 4, graph (d)]. The duration of the pulse has been chosen so that photobleaching of the activated molecules does not occur. Fitting of the plotted intensity values indicates that 488 nm photoactivation can be considered a linear process.

In conclusion, we experimentally demonstrated that the effective photoactivation spectrum of the paGFP molecule can be extended within the visible light region, indicating that photoactivation rates at observation wavelengths cannot be neglected in phototracking experiments. This observation is in tune with the broadening of the paGFP two-photon activation spectrum[4] indicating the existence of multiple energetic interactions leading to modifications of the chemical structure of the molecule and consequent alterations of its photophysical properties. We demonstrated the existence of an operative threshold allowing to maintain unaltered photophysical properties of native and activated paGFPs for a long time, consequently helping in setting the proper live cell imaging conditions to obtain unbiased data from biological samples.

Moreover, complete comprehension of the photophysics of the activation processes can help in better understanding the underlined conformational changes at molecular level, providing the basis and operative tools for applications of photoactivatable GFPs exploiting, for example, their photophysical plasticity to create biosensors.[10]

[1] J. Lippincott-Schwartz, N. Altan-Bonnet, and G. H. Patterson, Nat. Cell Biol. **7**, 14 (2003).
[2] G. H. Patterson and J. Lippincott-Schwartz, Methods **32**, 445 (2004).
[3] G. H. Patterson and J. Lippincott-Schwartz, Science **297**, 1873 (2002).
[4] M. Schneider, S. Barozzi, I. Testa, M. Faretta, and A. Diaspro, Biophys. J. **89**, 1346 (2005).
[5] M. Karbowski, J. Cell Biol. **164**, 493 (2004).
[6] J. N. Post, K. A. Lidke, B. Rieger, and D. J. Arndt-Jovin, FEBS Lett. **579**, 325 (2005).
[7] D. A. Stark and P. M. Kulesa, Dev. Dyn. **233**, 983 (2005).
[8] J. Beaudouin, F. Mora-Bermudez, T. Klee, N. Daigle, and J. Ellenberg, Biophys. J. **90**, 1878 (2006).
[9] S. Habuchi, R. Ando, P. Dedecker, W. Verheijen, H. Mizuno, A. Miyawaki, and J. Hofkens, Proc. Natl. Acad. Sci. U.S.A. **102**, 9511 (2005).
[10] J. W. Choi, Y. S. Nam, W. H. Lee, D. Kim, and M. Fujihira, Appl. Phys. Lett. **79**, 1570 (2001).